

Enhancement of penetration field in vortex matter in mesoscopic superconductors due to Andreev bound states

M. I. Dolz,¹ N. R. Cejas Bolecek,² J. Puig,² H. Pastoriza,² G. Nieva,² J. Guimpel,² C. J. van der Beek,³ M. Konczykowski,⁴ and Y. Fasano²

¹*Departamento de Física, Universidad Nacional de San Luis and CONICET, San Luis 5700, Argentina*

²*Centro Atómico Bariloche and Instituto Balseiro, CNEA, CONICET and Universidad Nacional de Cuyo, Bariloche 8400, Argentina*

³*Centre de Nanosciences et de Nanotechnologies, CNRS, Université Paris-Sud, Université Paris Saclay, Palaiseau 91120, France*

⁴*Laboratoire des Solides Irradiés, CEA/DRF/IRAMIS, Ecole Polytechnique, CNRS, Institut Polytechnique de Paris, Palaiseau 91128, France*



(Received 24 April 2019; revised manuscript received 6 July 2019; published 12 August 2019)

We study the field for the penetration of a first vortex, H_p , for vortex matter nucleated in micron-sized samples with edges aligned along the nodal and antinodal directions of the d -wave superconducting order parameter of $\text{Bi}_2\text{Sr}_2\text{CaCu}_2\text{O}_{8-\delta}$. Here we present evidence that the H_p for vortex matter nucleated in mesoscopic samples with edges parallel to the nodal direction is larger than for the antinodal case, $\sim 72\%$ at low temperatures. This finding supports the theoretical proposal that surface Andreev bound states appearing in a sample with edges parallel to the nodal direction would produce an anomalous Meissner current that increases the Bean-Livingston barrier for vortex penetration.

DOI: [10.1103/PhysRevB.100.064508](https://doi.org/10.1103/PhysRevB.100.064508)

I. INTRODUCTION

Nucleating crystals with one-hundred vortices or less in micron-sized superconducting samples [1–5] is a model playground for studying the general problem of how the physical properties of condensed-matter systems [6–9] are affected by confinement and surface effects. Indeed, surface effects in vortex matter in mesoscopic samples affect its thermodynamic, structural, and magnetic properties [10–13]. For instance, due to surface barriers, the field at which the first vortex penetrates, H_p [14,15], can be larger than the lower critical field H_{c1} that depends only on the penetration depth λ and the coherence length ξ of the material. This effect becomes more relevant when the size of the superconductors is decreased to the mesoscopic scale [4,11] at which the geometry and surface quality of the edge of the samples also affect vortex penetration [16].

Surface barriers produce hysteretic behavior in the vortex magnetic response and can be of two types. Geometrical barriers are caused by the extra energy cost for flux entry produced by the local enhancement, close to the sample edge, of the otherwise uniform outer field H [17,18]. Bean-Livingston (BL) barriers arise from the competition between the Meissner current pushing the vortex inside the sample versus the attraction of the vortex towards the outer image vortex [19,20]. On increasing H , the former term dominates and vortices penetrate the sample. The temperature and thickness evolution of the ratio between the BL and geometrical barriers was theoretically studied for the case of an infinite strip [16].

Theoretical studies considering a generalization of the London model predict that nucleating vortices in d -wave superconductors presenting Andreev bound states (ABS) [21,22] can modify the BL surface barrier and then H_p [23]. ABS are surface states localized within a distance $\sim \xi$ from

the edge of the samples [22], of a few nanometers for high T_c 's. These zero-energy excitations appear if the sample edge is oriented along the nodal (N) direction of the d -wave superconducting parameter and generate an anomalous Meissner current running opposite to the supercurrents [23,24]. This produces a decrease in the net surface current for samples with edges parallel to the N direction that in turn enhances the BL barrier: the term pushing the vortex inside has a lesser magnitude but the attraction towards the outer antivortex remains unaltered. Therefore, a dependence of H_p on the crystal orientation of the sample edge is expected [24]. Although these theoretical works study the electrodynamics of vortex penetration considering the influence of both ABS and a gap suppression at the surface in the case of N samples, this approach has some shortcomings. First, since it relies on an extended London approach, the effect of the vortex nucleation process is disregarded, an effect that has been considered in Ginzburg-Landau studies [25] but in materials with isotropic order parameter. Second, the work of Ref. [24] studies the case of an ideal infinite normal-superconducting interface, a geometrical situation far away from real experimental cases. Furthermore, this theoretical approach may not accurately predict the quantitative value of H_p , but nevertheless is rather robust in suggesting that the crystal orientation of the sample edge in superconductors with anisotropic order parameters may alter this magnitude.

An attempt to observe the predicted difference in H_p for samples with edges oriented along the N and antinodal (AN) directions was performed in Ref. [26]. However, in the $\sim 200\text{-}\mu\text{m}$ -size rectangular samples studied in that work, the authors reported a tiny crystal-orientation enhancement of H_p . Nevertheless, these surface effects are expected to be magnified when dramatically decreasing the size of the vortex crystal since surface barriers increasingly dominate

over pinning when reducing the sample size. Therefore, in order to increase the chance of observing these effects, we decreased even further the size of the samples and microengineered them with techniques that allowed us to have sample edges that were rather smooth on the scale of the penetration depth. In this work, we study vortex crystals with 10^3 – 10^6 vortices and 10-to-1 % surface-to-volume ratio nucleated in micron-sized $\text{Bi}_2\text{Sr}_2\text{CaCu}_2\text{O}_{8-\delta}$ square thin plates. We study two sets of square plates, with edges aligned along the N and the AN directions of the d -wave order parameter. The typical samples resulting from our microengineering process are smooth at the scale of the penetration depth. We found that H_p is enhanced in N with respect to AN square thin plates of the same size, up to ~ 72 % at low temperatures. This result has been detected thanks to the virtuous combination of low-noise local magnetic techniques and the nucleation of vortices in mesoscopic samples.

II. EXPERIMENT

We microengineer the square thin plates from optimally doped $\text{Bi}_2\text{Sr}_2\text{CaCu}_2\text{O}_8$ macroscopic single crystals [27] with critical temperature $T_c = 90$ K. We start from rectangular macroscopic samples aligned with their edges parallel to the a (or b) crystalline direction, i.e., parallel to the N direction of the d -wave order parameter. Samples were fabricated by combining optical lithography and physical ion milling [5]. N square plates are obtained by aligning the optical-lithography mask such that their sides are roughly parallel to the macroscopic sample edge, with a misalignment smaller than 2° . In a similar fashion, AN square plates were fabricated rotating the lithography mask $45 \pm 4^\circ$ from the previous configuration; see the Supplemental Material [28]. We studied several N and AN samples with square sides $L = 20, 30,$ and $50 \mu\text{m}$, thicknesses $t \sim 2 \mu\text{m}$. The critical temperature of all studied square plates is the same as that of the parent macroscopic crystal, $T_c = 90$ K. Both square plates have a similar surface roughness of $(0.07\text{--}0.08 \pm 0.01) \mu\text{m}$, making them smooth in the scale of the penetration depth of $\sim 0.2 \mu\text{m}$ for low temperatures; see Supplemental Material [28]. Then, even though surface roughness can affect the BL barrier for vortex penetration [29], for the square plates studied here this effect is quite probably minor and has roughly the same magnitude for N and AN samples.

Figure 1 shows various samples placed on top of Hall sensors with $16 \times 16 \mu\text{m}^2$ working areas microfabricated from GaAs/AlGaAs heterostructures. Samples were micromanipulated and glued with Apiezon N grease to improve thermal contact. Local ac and dc magnetization measurements were performed applying dc, H , and ripple, $h_{ac} \ll H$, magnetic fields parallel to the c axis. The Hall sensor signal is proportional to the magnetization of the samples, $H_s = (B - H)$. We measure dc and ac hysteresis loops recording H_s and the sample transmittivity T' on sweeping H . T' is obtained applying an h_{ac} and normalizing the in-phase component of the first-harmonic signal, B' . This magnitude is measured by means of a digital-signal-processing lock-in technique using the lock-in reference signal as supply to the coil generating h_{ac} . The normalization $T' = [B'(T) - B'(T \ll T_c)]/[B'(T > T_c) - B'(T \ll T_c)]$ is such that $T' = 1$ in the normal state and

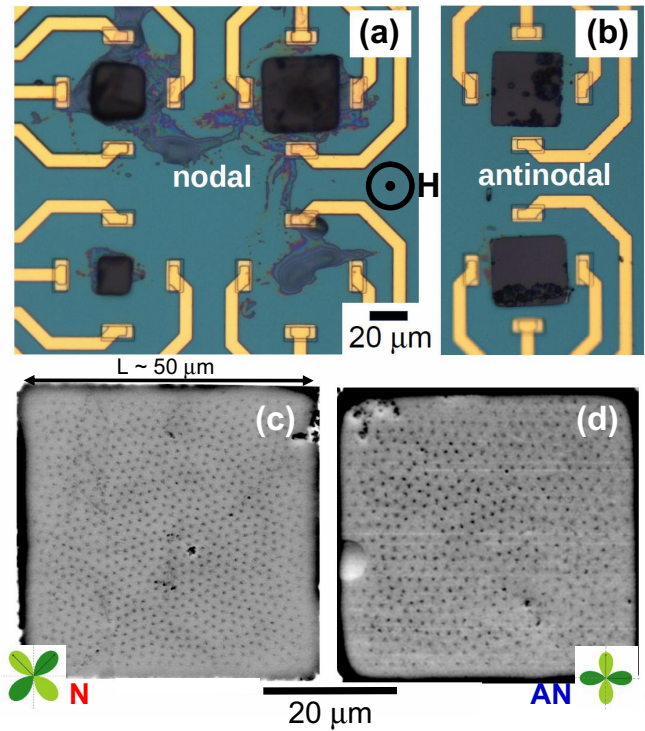


FIG. 1. Some of the nodal (N) and antinodal (AN) $\text{Bi}_2\text{Sr}_2\text{CaCu}_2\text{O}_{8+\delta}$ square thin plates studied located on top of $16 \times 16 \mu\text{m}^2$ Hall sensors. (a) N square plates with sides $L = 20, 30,$ and $50 \mu\text{m}$; (b) AN square plates with $L \sim 50 \mu\text{m}$. Vortex structure in mesoscopic samples imaged by magnetic decoration in (c) N (8.5 Gauss) and (d) AN (5 Gauss) square plates (see the orientation of the nodes of the d -wave superconducting parameter).

$T' = 0$ well within the superconducting phase. The h_{ac} ripple field applied in the ac experiments has a frequency of 7.1 Hz and a rms amplitude of 1 Oe.

III. RESULTS AND DISCUSSIONS

The superconducting quality of the square thin plates was checked by magnetic decoration experiments [30]. Figures 1(c) and 1(d) show vortex crystals nucleated in mesoscopic samples at low vortex densities in N (8.5 Gauss) and AN (5 Gauss) square plates with $L = 50 \mu\text{m}$. The black dots correspond to individual vortices decorated with magnetized Fe nanoparticles attracted to the cores due to their local field gradient. Regular vortex structures with an excess of topological defects induced by confinement [13] are observed for both N and AN square plates.

Figure 2(a) shows illustrative dc hysteresis loops at 54 K in N and AN square plates, both with $L = 50 \mu\text{m}$. On increasing the field from zero, H_s first follows the linear Meissner response associated to complete field expulsion. The entrance of the first vortex into the square plates is signposted by the departure of H_s from linearity, at a field H_p . On further increasing field, H_s changes curvature as expected when vortices penetrate. The dc loops have a two-quadrant structure with branches located mostly in the second and fourth quadrants. The two field-descending branches for positive and negative H are almost horizontal and close to zero. The same

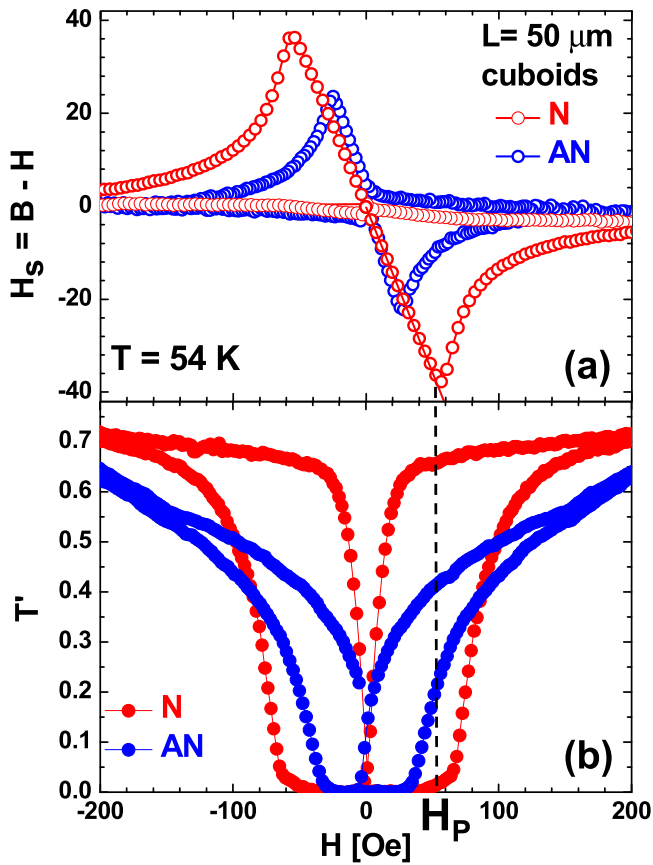


FIG. 2. Detection of the penetration field H_p in nodal (N) and antinodal (AN) square plates (with $L = 50 \mu\text{m}$) from (a) dc and (b) ac magnetic hysteresis loops. The H_p determined from the deviation of the linear Meissner response coincides with the field at which transmittivity becomes non-negligible (see vertical dashed lines). Measurements performed at 54 K; ac measurements with h_{ac} of 1 Gauss and 7.1 Hz.

behavior is observed for all dc loops measured between 35 and 90 K; see Supplemental Material [28]. This phenomenology suggests that bulk pinning has a lesser effect than surface barriers for vortex penetration in our superconducting square plates.

We also measured H_p in N and AN square plates from ac hysteresis loops; see Fig. 2(b) for the case of 54 K. At low fields, $T' = 0$, indicating full expulsion of the magnetic field; on increasing field, T' becomes non-negligible at roughly the same H_p where the departure of linearity is detected in dc loops; see dashed line in Fig. 2. On further increasing H , the number of vortices penetrating the sample enhances and T' grows in accordance, reaching a value close to 1 for high fields. For a given H , T' in the descending branch is larger than in the ascending one since in the former there is extra trapped flux.

The most remarkable result of the dc and ac data of Fig. 2 is that the penetration field for N is larger than for AN square plates. Figure 3(a) shows a comparison between the temperature evolution of H_p for N and AN square plates with $L = 50 \mu\text{m}$. Data points were obtained averaging data in two pairs of N and AN square plates and error bars come from

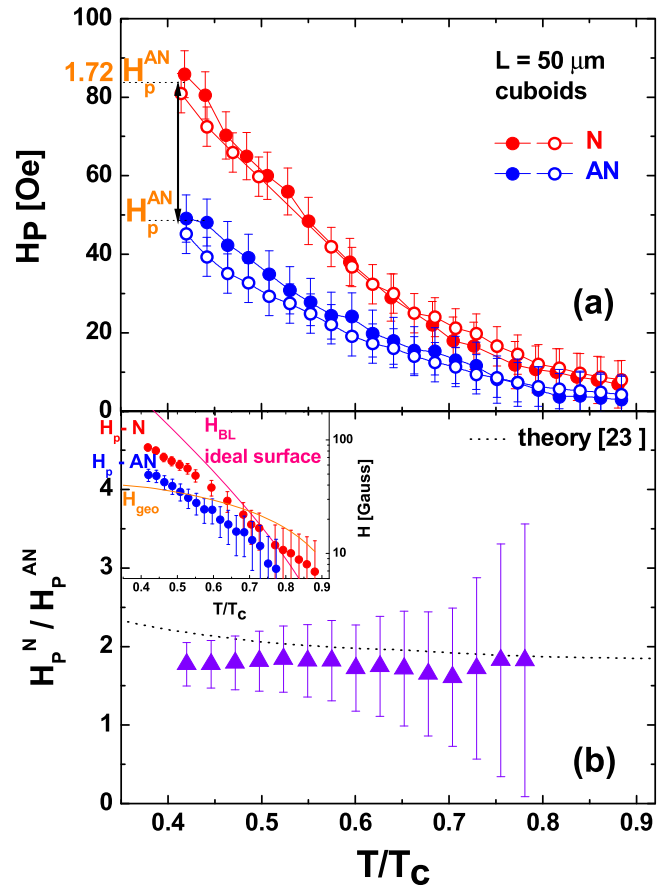


FIG. 3. (a) Temperature dependence of the penetration field H_p for nodal (N) and antinodal (AN) square plates from dc and ac (open and full symbols) measurements. (b) H_p^N/H_p^{AN} data (symbols) and temperature dependence predicted theoretically in Ref. [24] (black dotted line) for a superconductor with $\kappa = 200$. This line is just the digitalization of the data shown in Fig. 3 of Ref. [24]. Inset: Data of (a) compared with the theoretical expectation for geometrical (orange) and BL (pink) barriers for $\text{Bi}_2\text{Sr}_2\text{CaCu}_2\text{O}_{8+\delta}$ disks with radius L .

the dispersion in the different samples. The values obtained considering the virgin branches of ac (open points) and dc (full points) magnetization loops are similar within the uncertainty. In all the studied temperature range, H_p^N is larger than H_p^{AN} beyond error bars, with this difference increasing on cooling. For instance, for the smallest measured temperature, $T/T_c \sim 0.4$, $H_p^N \simeq 1.72H_p^{AN}$.

Even though H_p is sensitive to the side of the square plates, this difference cannot be accounted for by the eventual small changes in L . Figure 4 shows the temperature dependence of H_p for N square plates with $L = 20, 30,$ and $50 \mu\text{m}$. The smaller the L , the larger H_p , but the separation between the curves enlarges on decreasing T . In particular, at $T/T_c \sim 0.4$, the H_p difference between the 20 and $50 \mu\text{m}$ square plates is $\sim 15\%$, much smaller than that found between H_p^{AN} and H_p^N at the same T .

We calculated the ratio H_p^N/H_p^{AN} by averaging H_p data obtained from ac and dc measurements; see Fig. 3(b). This ratio seems to be featureless in temperature, even if the error bars are significant. The figure also shows with a dotted

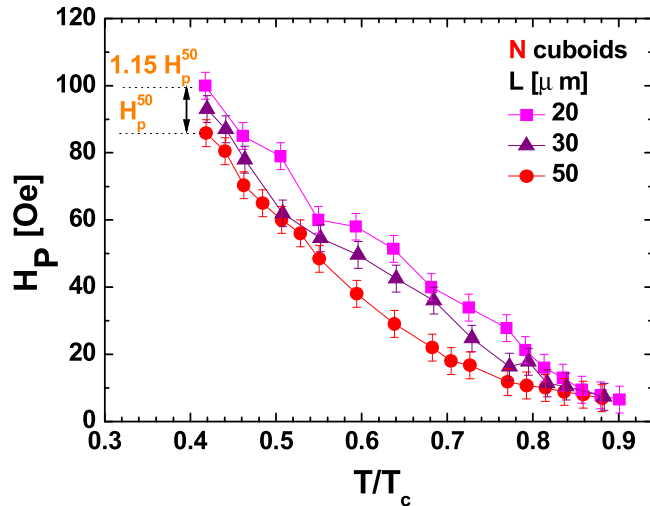


FIG. 4. Temperature dependence of the penetration field for nodal square plates with different square sides of $L = 20, 30$, and $50 \mu\text{m}$. Data from ac magnetization (h_{ac} of 1 Gauss rms and 7.1 Hz) in agreement with dc data within the error.

line the theoretically expected evolution of H_p^N/H_p^{AN} when considering the effect of Andreev bound states in the BL surface barrier for an ideal infinite sample of a d -wave superconductor with $\kappa = \lambda/\xi = 200$, and neglecting any other barrier for vortex penetration [24]. This line is just the digitalization of the data shown in Fig. 3 of Ref. [24]. For the vortex crystals studied here, $\kappa \sim 200$ as in the theoretical study, but the square plates are not an ideal infinite interface. Nevertheless, the accordance between our experimental data and the theoretically predicted evolution of Ref. [24] with no adjustable parameters is quite remarkable. On the other hand, our N and AN experimental data are not so far to the penetration field expected theoretically when considering the BL barrier in a square thin plate superconductor with an isotropic order parameter, i.e., not taking into account the effect of the Andreev bound states; see pink curve in the inset to Fig. 3(b) calculated for the case of $L = 50 \mu\text{m}$ and $t = 2 \mu\text{m}$. This curve was obtained considering that the temperature dependence of H_p for a BL barrier in an ideally specular surface of an s -wave superconductor is $H_{BL}(T) = H_c(T)\sqrt{t/L} \exp(-T/T_0)$ [4,20,31]. $H_c(T) \simeq \kappa H_{c1}(T)/\ln \kappa$ is the thermodynamic critical field with $H_{c1}(T)$ the first critical field, and $T_0 \sim 15 \text{ K}$ for $\text{Bi}_2\text{Sr}_2\text{CaCu}_2\text{O}_8$ [4], a characteristic temperature below which thermally activated vortex creep is irrelevant [4,20,31]. This ideal $H_{BL}(T)$ coincides with the data at high T , and overpasses them by more than a factor of

two at low T . This discrepancy quite likely has its origin in the nonideal nature of the edges of our samples.

Nevertheless, the H_p^N/H_p^{AN} experimental data lay pretty close to the theoretical value expected when considering the effect of Andreev bound states, even though this theoretical curve has no other free parameter than the κ of the superconducting material. In addition, geometrical barriers do not seem to play a relevant role at $T/T_c \lesssim 0.6$ to explain the enhancement of H_p^N versus that of H_p^{AN} . Indeed, the inset to Fig. 3(b) shows that H_{geo} , an estimation of the penetration field associated to the geometrical barrier for mesoscopic samples, is well below the experimental data for $\text{Bi}_2\text{Sr}_2\text{CaCu}_2\text{O}_{8+\delta}$ square plates at low temperatures and, in addition, has a different temperature evolution. This estimative curve is obtained considering that $H_{geo} = H_{c1}(T) \tanh \sqrt{0.67t/L}$, with 0.67 the geometrical factor for a disk geometry with diameter L approximating our square plates [32].

IV. CONCLUSIONS

In conclusion, the comparison between the theoretical BL and geometrical barriers in square plates, and our experimental data in square plates of a d -wave superconductor, suggests the dominance of the BL barrier for vortex penetration at low T . This can be at the origin of the rather good quantitative agreement between the experimental data and the theoretically predicted H_p^N/H_p^{AN} for d -wave ideal infinite superconductors, a striking result considering that this theoretical calculation depends only on the value of ξ for the superconducting material. The latter suggests that the barriers for vortex penetration in N square plates are fully governed by the decrease in the effective Meissner current induced by the presence of Andreev bound states located only up to a distance $\xi \sim 5 \times 10^{-4}L$ from the surface of the square plates. Therefore, we present here evidence of a phenomena in the magnetic properties of vortex crystals nucleated in mesoscopic samples emergent from the microscopic local electronic properties of anisotropic d -wave superconductors. From an applied point of view, our data suggest that the crystal orientation of micron-sized samples made of high T_c 's with anisotropic order parameters is a property that has to be taken into account for the magnetic response of devices based in such tiny building blocks.

ACKNOWLEDGMENTS

We thank V. Mosser for providing the sensors and M. Li for growing the macroscopic crystals. Financial support was provided by Grants No. ECOS-Sud Argentina-France A14E02, No. ANR-10-LABX-0039-PALM, and No. ANR-CE08-007 DiSSCo-Hall.

[1] V. V. Moshchakov, L. Gielen, C. Strunk, R. Jonckheere, X. Qiu, C. Van Haesendonck, and Y. Bruynseraede, *Nature (London)* **373**, 319 (1995).
 [2] A. K. Geim, I. V. Grigorieva, S. V. Dubonos, J. G. S. Lok, J. C. Maan, A. E. Filippov, and F. M. Peeters, *Nature (London)* **390**, 259 (1997).
 [3] V. A. Schweigert, F. M. Peeters, and P. S. Deo, *Phys. Rev. Lett.* **81**, 2783 (1998).

[4] Y. M. Wang, M. S. Fuhrer, A. Zettl, S. Ooi, and T. Tamegai, *Phys. Rev. Lett.* **86**, 3626 (2001).
 [5] M. I. Dolz, Y. Fasano, N. R. Cejas Bolecek, H. Pastoriza, V. Mosser, M. Li, and M. Konczykowski, *Phys. Rev. Lett.* **115**, 137003 (2015).
 [6] C. J. Coombes, *J. Phys. F: Metal Phys.* **2**, 441 (1972).
 [7] A. N. Goldstein, C. M. Echer, and A. P. Alivisatos, *Science* **256**, 1425 (1992).

- [8] S. H. Tolbert and A. P. Alivisatos, *Science* **265**, 373 (1994).
- [9] G. Guisbiers and L. Buchaillot, *Phys. Lett. A* **374**, 305 (2009).
- [10] J. J. Palacios, *Phys. Rev. B* **58**, R5948 (1998).
- [11] M. I. Dolz, Y. Fasano, N. R. Cejas Bolecek, H. Pastoriza, M. Konczykowski, and C. J. van der Beek, *J. Phys.: Conf. Ser.* **568**, 022010 (2014).
- [12] N. R. Cejas Bolecek, M. I. Dolz, A. Kolton, H. Pastoriza, C. J. van der Beek, M. Konczykowski, M. Menghini, G. Nieva, and Y. Fasano, *J. Low Temp. Phys.* **179**, 35 (2015).
- [13] N. R. Cejas Bolecek, M. I. Dolz, H. Pastoriza, M. Konczykowski, C. J. van der Beek, A. B. Kolton, and Y. Fasano, *Phys. Rev. B* **96**, 024507 (2017).
- [14] M. Konczykowski, L. I. Burlachkov, Y. Yeshurun, and F. Holtzberg, *Phys. Rev. B* **43**, 13707(R) (1991).
- [15] J. R. Clem, *J. Supercond. Nov. Magn.* **21**, 343 (2008).
- [16] E. H. Brandt, G. P. Mikitik, and E. Zeldov, *J. Expt. Theor. Phys.* **117**, 439 (2013).
- [17] E. Zeldov, A. I. Larkin, V. B. Geshkenbein, M. Konczykowski, D. Majer, B. Khaykovich, V. M. Vinokur, and H. Shtrikman, *Phys. Rev. Lett.* **73**, 1428 (1994).
- [18] R. Willa, V. B. Geshkenbein, and G. Blatter, *Phys. Rev. B* **89**, 104514 (2014).
- [19] A. E. Koshelev, *Physica C (Amsterdam)* **191**, 219 (1992).
- [20] L. Burlachkov, *Phys. Rev. B* **47**, 8056 (1993).
- [21] M. Fogelström, D. Rainer, and J. A. Sauls, *Phys. Rev. Lett.* **79**, 281 (1997).
- [22] C.-R. Hu, *Phys. Rev. Lett.* **72**, 1526 (1994).
- [23] C. Iniotakis, S. Graser, T. Dahm, and N. Schopohl, *Phys. Rev. B* **71**, 214508 (2005).
- [24] C. Iniotakis, T. Dahm, and N. Schopohl, *Phys. Rev. Lett.* **100**, 037002 (2008).
- [25] A. D. Hernández and D. Domínguez, *Phys. Rev. B* **65**, 144529 (2002).
- [26] A. E. Böhmer, M. Konczykowski, and C. J. van der Beek, [arXiv:1004.5309v1](https://arxiv.org/abs/1004.5309v1).
- [27] T. W. Li, P. H. Kes, N. T. Hien, J. J. M. Franse, and A. A. Menovsky, *J. Cryst. Growth* **135**, 481 (1994).
- [28] See Supplemental Material at <http://link.aps.org/supplemental/10.1103/PhysRevB.100.064508> for further details in the preparation of N and AN square plates, as well as the temperature evolution of dc magnetization loops.
- [29] F. Bass, V. D. Freilikher, B. Ya. Shapiro, and M. Shvaster, *Physica C (Amsterdam)* **260**, 231 (1996).
- [30] Y. Fasano, J. Herbsommer, and F. de la Cruz, *Phys. Status Solidi B* **215**, 563 (1999).
- [31] V. N. Kopylov, A. E. Koshelev, I. F. Schegolev, and T. G. Togonidze, *Physica C (Amsterdam)* **170**, 291 (1990).
- [32] E. H. Brandt, *Phys. Rev. B* **60**, 11939 (1999).